Journal of Electronics, Electromedical Engineering, and Medical Informatics
Homepage: jeeemi.org; Vol. 8, No. 1, January 2026, pp: 105-118 e-ISSN: 2656-8632

RESEARCH ARTICLE

OPEN ACCESS

Graph-Theoretic Analysis of Electroencephalography Functional Connectivity Using Phase Lag Index for Detection of Ictal States

Ghansyamkumar Rathod, Hardik Modi

Department of Electronics and Communication, Chandubhai S Patel Institute of Technology, Charotar University of Science and Technology, Gujarat, India

Corresponding author: Ghansyamkumar Rathod (e-mail: 17drec016@charusat.edu.in), **Author(s) Email**: Hardik Modi (e-mail:hardikmodi.ec@charusat.ac.in)

Abstract **Epileptic disorders are characterized by the misfiring of neurons and affect 50 million people worldwide, who have to live with physical challenges in their normal lives. The ionic activity of the brain can be detected as an electrical activity from the scalp using a non-invasive bio-potential measurement technique known as electroencephalography (EEG). Manual interpretation of brainwaves is a time-consuming, expert-intensive task. In recent years, AI has achieved remarkable results, but at the cost of large datasets and high processing power. We used publicly available online datasets from the Children's Hospital Boston (CHB) in collaboration with the Massachusetts Institute of Technology (MIT). The datasets consisted of 23 bipolar channels that included pre-processed epochs of both normal and pre-labeled seizure (ictal) states. Using the Phase Lag Index (PLI), the functional connectivity of the network was built to record consistent phase synchronization while minimizing artifacts from volume conduction. Graph-theory-based features were used to detect the brain's seizure state. A significant increase in the values of graph theoretical features, such as degree centrality and clustering coefficient, was observed, along with the formation of hyper-connected hubs and disrupted brain communication in the ictal state. Statistical tests (T-tests, ANOVA, Mann-Whitney U) across multiple PLI thresholds confirmed consistent significant differences (p-value < 0.05) between normal and ictal conditions. This study aims to provide a method based on graph theory, which is computationally efficient, interpretable, and suitable for real-time seizure detection. Considering the efficiency of clustering coefficient and degree of centrality, we can say that they are useful biomarkers for biomedical applications.**

Keywords **Phase Lag Index (PLI), Graph Theory, Electroencephalography (EEG), Seizure or Ictal state, Clustering coefficient, Degree Centrality**

I. Introduction

Neurological activity can be detected from the human scalp using a non-invasive method known as electroencephalography (EEG), where surface electrodes are placed on the scalp using a 10-20 EEG measurement system at predetermined intervals. Raw data were captured and recorded for further analysis. Owing to their high temporal resolution, EEGs are widely used worldwide. The EEG method is helpful for diagnosing neurological disorders. Misfiring of neurons can cause disturbances in the routine activities of a person, known as epilepsy or seizure attacks. According to the World Health Organization (WHO), nearly 50 million people are affected by epilepsy. It can be further defined as the recurrence of spontaneous and unprovoked seizures resulting from abnormal and excessive neuronal discharge. Epileptic seizures can manifest as lapses of attention or muscle jerks, or severe convulsions. This has a significant impact on quality of life [1], [2]. Epilepsy is classified into several categories. One is a focal seizure that originates in a localized brain region. The other type is generalized seizures, which involve both hemispheres simultaneously, and the remaining is the combined or unknown type, where classification remains unclear due to overlapping features. The identification and prediction of seizure episodes are crucial not only for clinical intervention but also for improving long-term patient care [3], [4].

EEG provides significant results in both ictal (seizure) and interictal (non-seizure) states of the brain. Raw EEG signals are often contaminated with artifacts, such as muscle activity, eye blinks, and power-line interference; therefore, preprocessing is essential. Filtering techniques, such as band-pass filters to retain the relevant frequency bands (0.5 to 40 Hz), notch filters to suppress 50 or 60 Hz power line noise, and

Manuscript received 29 September 2025; Revised 27 November 2025; Accepted 25 November 2025; Available online 10 December 2025
Digital Object Identifier (**DOI**): https://doi.org/10.35882/jeeemi.v8i1.1230

motion artifact removal, were used. Once the filtering is completed, the signals are more reliable for further analysis, allowing better extraction of the underlying informative features derived from PLI-based connectivity networks. Degree centrality provides insight into the relationships between a node (EEG

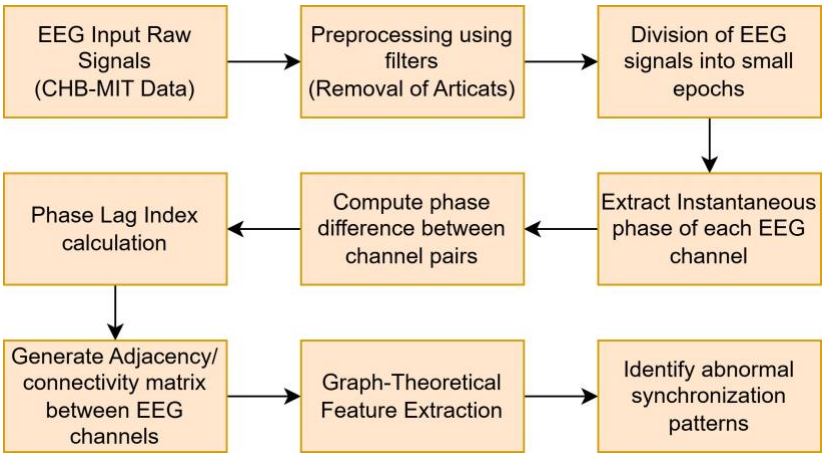

Fig. 1. Block diagram of the proposed method shows data filtering from raw data and preprocessed for feature extraction

neurological information associated with epileptic activity [5], [6], [7]. In recent years, network-based methods have become increasingly important for seizure detection. One such measure is the Phase Lag Index (PLI), which quantifies the consistency of the phase differences between pairs of EEG signals. Unlike traditional articulacy methods, PLI reduces the ascendancy of common sources and volume conduction, making it a robust measure for functional connectivity analysis [4], [8].

PLI provides a core understanding of neural communication, which is disrupted by epileptic seizures owing to the directional and nonlinear interactions between non-identical brain regions. Moreover, degree centrality and clustering coefficient are two highly channel or brain region) and other nodes that may act as epileptic hubs. The clustering coefficient quantifies the nature of nodes to form local clusters and provides more insight into the separation and synchronization patterns of the network. Any abnormalities in these two features can be directly correlated with epileptic seizures, providing reliable markers for automatic seizure detection systems [2], [9].

The approach we used to detect the ictal state began with raw EEG signals, which were preprocessed to remove artifacts for further analysis. The preprocessed data were divided into small epochs of ictal and normal states, considering the labeling provided by the data providers. The next stage is the extension of the instantaneous phase of the EEG

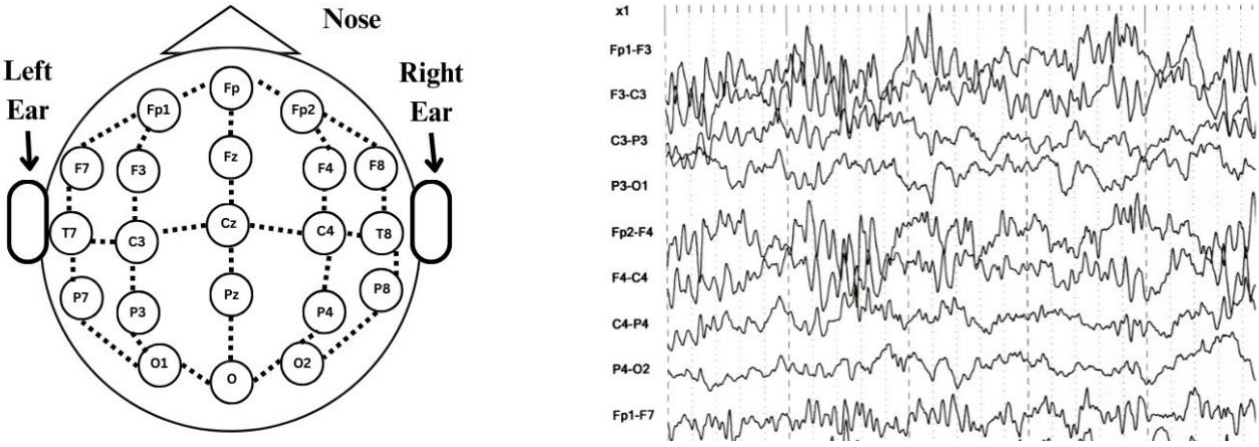

(a) (b)

Fig. 2. Topographic View and EEG (a) Electrode Placements on scalp using 10-20 EEG Method. (b) Sample EEG waveform of Bipolar Montage Channels.

Manuscript received 29 September 2025; Revised 27 November 2025; Accepted 25 November 2025; Available online 10 December 2025
Digital Object Identifier (**DOI**): https://doi.org/10.35882/jeeemi.v8i1.1230

channel, and the computation of phase differences for PLI calculations is performed. Finally, the connectivity matrix generation and feature extraction process were completed to detect the normal and ictal states of the brain to detect the epileptic seizure, as shown in the block diagram in Fig. 1 [8], [10], [11].

A. The AIM of the study

1. To demonstrate a computationally effective and interpretable algorithm for epileptic seizure detection using electroencephalography signals.
2. To create functional brain networks from EEG recordings based on the Phase Lag Index (PLI) and biomarkers of functional connectivity while reducing volume conduction effects.
3. To fetch and analyze graph-theoretic features, specifically the degree centrality and clustering coefficient, across different PLI thresholds to distinguish between normal and ictal brain states.
4. To statistically validate the significance of the extracted features, tests such as the t-test, ANOVA, and the Whitney U test were applied to confirm their discriminative power.
5. To show Graph-based features derived from PLI-based networks can serve as reliable biomarkers for seizure detection, enabling simpler and more interpretable models than conventional machine learning or deep learning approaches.

To detect epileptic seizures, the datasets used in this study were publicly available from Children's Hospital Boston in association with the Massachusetts Institute of Technology (CHB-MIT). These EEG datasets are particularly suitable for the proposed method because they provide long-term, multi-channel EEG recordings with well-annotated ictal and non-ictal states, enabling direct comparison between seizure and normal brain activity. The datasets available include 23 bipolar channels, sampled at 256 Hz, which is sufficient for high spatial and temporal resolution. Fig. 2 depicts the top view of the Electrodes and the EEG waveform, where (a) shows the Electrode placement on the human scalp using the 10-20 measurement system, and (b) shows the EEG waveforms in the time domain. Higher spatial and temporal resolutions are suitable for constructing functional connectivity networks using the Phase Lag Index (PLI). The presence of multiple seizure episodes across different patients ensures the robust validation of graph-theoretical features, such as degree centrality and clustering coefficient, which are strong biomarkers of network-level alterations in brain communication during seizures. Additionally, the huge volume of data supports reliable statistical testing, making CHB-MIT a benchmark dataset for developing and evaluating real-time seizure detection techniques [12], [13], [14], [15].

II. Method

This study was based on the datasets provided by CHB-MIT, which were anonymized and hosted online on PhysioNet. Ethical approval for this study was not required because the CHB-MIT dataset was previously collected under ethical protocols approved by the Institutional Review Board (IRB) of Boston Children's Hospital and the Massachusetts Institute of Technology. All the data were collected in accordance with the principles of the Declaration of Helsinki. The CHB-MIT dataset was collected with the necessary information and patient or legal guardian consent. As secondary users of these open-access data, we affirm that our research complies with all applicable institutional, national, and international ethical standards, including the Declaration of Helsinki. From the CHB-MIT database, a few results are shown for the respective subjects, which include a mix of seizure and non-seizure (ictal and interictal) events across different ages and genders.

The dataset's rich temporal resolution, with a sampling frequency of 256 Hz, 23-channel configuration, and documented seizure onset times, makes it suitable for graph-theoretical EEG analysis and seizure detection studies. EEG recordings with clearly labeled seizure events (ictal periods), along with availability of both seizure and normal (non-ictal) states, bipolar montage recording with 23 EEG channels, and a sampling frequency of 256 Hz. Missing channel data for any subject or incomplete EEG recordings. Recording annotated seizure onset and offset, corrupted or low-quality EEG signals due to excessive artifacts. The data used in this study are openly available in the PhysioNet repository: CHB-MIT Scalp EEG Database [https://physionet.org/content/chbmit/1.0.0/]. These data were used in compliance with the PhysioNet data use agreement. The primary stage of working with EEG data is to filter the raw data and extract appropriate epochs. The selected raw data were converted to comma-separated value (Comma Separated Value) files from the European Data Format (EDF). Each CSV file can be extracted from the open-source browser, EDF browser, available online. The CSV file channel headers were maintained, and there were 23 channels in total.

The EEG signals were acquired using bipolar montages. The preprocessing of such raw signal epochs was performed using a band-pass filter and a notch filter to remove the power line noise. The epoch at a specific time interval can be represented by Eq. (1) [35].

$$\tilde{x}_i(t) = \mathrm{BP}_{f_1,f_2}\{x_i(t)\} \quad (1)$$

Each epoch $\tilde{x}_i(t)$ (channel i) is bandpass filtered to the relevant frequencies (f_1, f_2) band (1-40Hz) using a zero-phase FIR filter as shown in Eq. (1). The

Manuscript received 29 September 2025; Revised 27 November 2025; Accepted 25 November 2025; Available online 10 December 2025
Digital Object Identifier (**DOI**): https://doi.org/10.35882/jeeemi.v8i1.1230

powerline noise can be removed using a notch filter at 50 Hz and 60 Hz frequencies. To remove transient artifacts, we apply an automated z-score criterion as shown in Eq. (2) [35].

$$z_i(t) = \frac{\tilde{x}_i(t) - \mu_i}{\sigma_i} \quad (2)$$

where, μ_i and σ_i are the mean and standard deviation of $\tilde{x}_i(t)$. The independent component analysis (ICA) can also be used to remove ocular/muscular signals before reconstruction of the required signals, and that can be denoted by $s_i(t)$.

The selection of the equal time length epochs for ictal and normal periods is done using the annotation by the data provider for further processing. The instantaneous phase extraction from the cleaned signal can be done using the Hilbert transform $\mathcal{H}\{\cdot\}$. The amplitude of the channel i at time t, can be represented by Eq. (3) [35].

$$\mathcal{A}_i(t) = s_i(t) + j\mathcal{H}\{s_i(t)\} = R_i(t)e^{j\phi_i(t)} \quad (3)$$

where, $\phi_i(t) = \arg(\mathcal{A}_i(t))$ is the instantaneous phase for the channel i. The functional connectivity between different brain regions can be measured using the Phase Lag Index (PLI) from EEG signals. It compares and quantifies the consistency of the phase differences between two EEG channels over time. Compared with simple correlations, the PLI is designed to lower the effect of volume conduction [8]. Mathematically, for two EEG signals/channels $i(t) and\, j(t)$, their instantaneous phases $\Delta\phi_{ij}(t)$ can be computed using the Hilbert transform. The phase difference can be calculated using Eq. (4) [35].

$$\Delta\phi_{ij}(t) = \phi_i(t) - \phi_j(t) \quad (4)$$

PLI can be represented mathematically using Eq. (5) [24].

$$\mathrm{PLI}_{ij} = \left|\frac{1}{T}\sum_{t=1}^{T} \mathrm{sign}\big(\sin(\Delta\phi_{ij}(t))\big)\right| \quad (5)$$

where, T is the number of samples, $sign(x) = 1\, for\, x > 0, 0\, for\, x = 1\, and\, -1\, for\, x < 0$. Intuitively, PLI measures the consistency of non-zero phase lead/lag between two signals. PLI reduces zero-lag coupling effects (volume conduction) because zero-lag phase differences contribute near zero to $\sin(\Delta\phi)$ and so do not bias the sign average. A PLI value close to zero indicates a non-consistent phase relationship, and a value close to one indicates a strong phase locking. Abnormal synchronization in brain networks occurs due to epileptic seizures, and because of this, the PLI is highly suitable for epilepsy detection. The PLI reduces false connectivity due to volume conduction and provides only meaningful phase relationships, which makes it more robust than coherence or correlation measures [16].

The connectivity between all EEG channels can be obtained using the PLI matrix, which can be represented by a graph. In the graph, the brain region is represented by nodes, and edges indicate PLI values or connectivity strengths. The PLI plays an important role in brain studies. As far as epilepsy is concerned, it is useful to identify seizure-related synchronization between brain regions. In Alzheimer's disease, PLI reveals network disconnections and reduced synchronization, whereas in schizophrenia, PLI is useful for studying abnormal connectivity patterns. Sleep research is useful in identifying changes in connectivity across sleep stages and for Parkinson's disease to obtain statistics on motor network abnormalities. The PLI is also useful in the brain–computer interfaces (BCI) for classifying mental tasks. These applications enhance the reliability and robustness of PL, as well as its versatility in understanding brain dynamics [8], [17], [18].

There are multiple reasons for selecting PLI for our study, including its computational efficiency, robustness in artifacts, and capability of capturing synchronization, which is a benchmark for detecting seizures. The construction of the graph and thresholding is based on the Adjacency matrix defined in Eq. (6) [24].

$$A_{ij}^{(\tau)} = \begin{cases} 1, & PLI_{ij} \geq \tau, \\ 0, & PLI_{ij} < \tau. \end{cases} \quad (6)$$

where, τ is the threshold values. We utilized the values of thresholds $\tau \in \{0.05, 0.1, 0.15\}$ where 0.05 indicates weak but potentially meaningful synchronizations. It was sensitive but less specific. The threshold value of 0.1 is a moderate cutoff commonly used in the EEG-PLI literature to balance noise removal and signal retention. The threshold value of 0.15 is a strict cutoff that highlights only the strongest and most robust connections (improving specificity). We analyzed features across these thresholds to ensure that the results were robust and not dependent on a single threshold.

The features degree centrality and clustering coefficient were chosen because they directly reflect network-level alterations along with the formation of seizure-related hubs and excessive local connectivity. All the properties of PLI provide a suitable framework for identifying seizures in real time [19], [20].

A. Feature Extraction

After the PLI connectivity matrix is computed for the EEG channels, it can be treated as a graph, with the channels represented as nodes and the edges representing the synchronization strength. From these graphs, two key features can be extracted. Degree Centrality can be calculated using Eq. (7) [22].

$$DC(i) = \sum_{j=1}^{N} A_{ij} \quad (7)$$

where, A_{ij} is the adjacency matrix of the PLI values. This value of N indicates the strength of the connection between a node or brain region and other nodes or

Manuscript received 29 September 2025; Revised 27 November 2025; Accepted 25 November 2025; Available online 10 December 2025
Digital Object Identifier (**DOI**): https://doi.org/10.35882/jeeemi.v8i1.1230

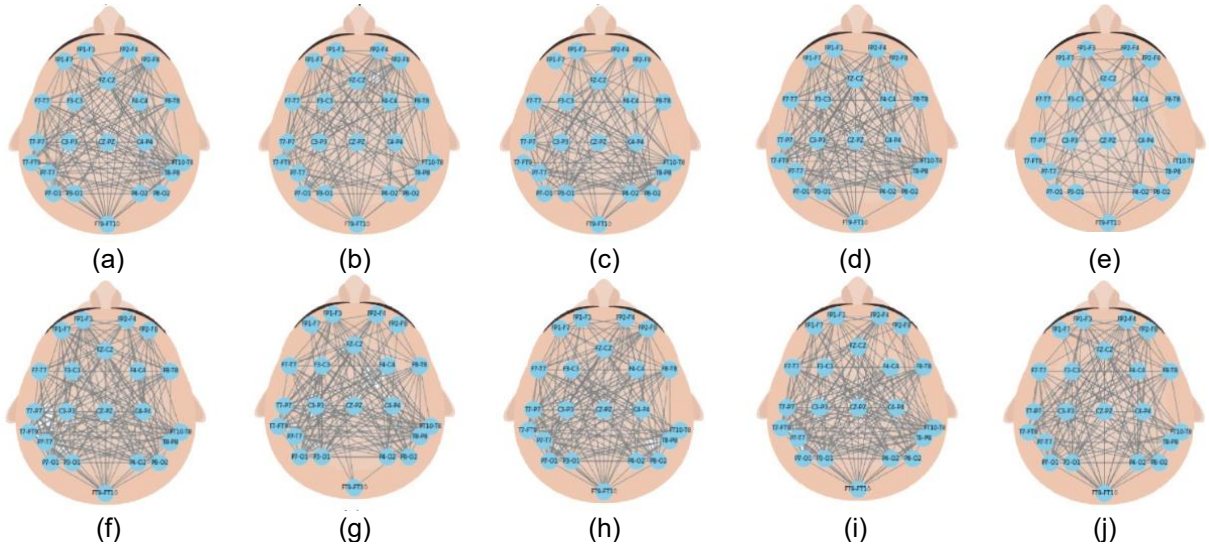

Fig. 3. PLI Graphs threshold level 0.1 Normal state for (a) Sample 1, (b) Sample 2, (c) Sample 3, (d) Sample 4, (e) Sample 5. PLI Graphs threshold level 0.1 Ictal state for (f) Sample 1, (g) Sample 2, (h) Sample 3, (i) Sample 4, (j) Sample 5

brain regions. Abnormal hubs with high connectivity often emerge during seizure episodes. The Clustering Coefficient can be calculated using Eq. (8) [22].

$$C(i) = \frac{2e_i}{k_i(k_i-1)} \quad (8)$$

where, k_i is the number of neighbors of the node i & e_i is number of edges between the neighbors of the node i. This measures how densely connected a node's neighbors are, indicating excessive local clustering in seizure states. Fig. 3. shows the PLI-based functional connectivity graph for a threshold value of 0.1. The top five figures (a) to (e) show the PLI graphs of the normal brain state for samples 1 to 5, whereas the bottom figures (f) to (j) show the PLI graphs of the ictal brain state for samples 1 to 5. Nodes are Bipolar channels placed on an approximate scalp topography, where edges denote suprathreshold PLI connections. We observed that ictal networks were visually denser and more locally clustered than normal networks, consistent with the higher average degree centrality and clustering coefficient measured in our analysis.

B. Statistical Analysis

The significance of our statistical validation was determined based on the p-values from the Mann-Whitney U test, Analysis of Variance (ANOVA), and T-tests. The independent two-sample t-test can be done using Eq. (9) [36].

$$t = \frac{\bar{x}_1 - \bar{x}_2}{\sqrt{\frac{s_1^2}{n_1} + \frac{s_2^2}{n_2}}} \quad (9)$$

With a degree of freedom approximated by Welch's formula if the variances differ. Here $\bar{x}_i, s_i^2, n_i$ denote the sample mean, variance, and sample size for the group i. The Mann-Whitney U test to get the U statistics can be done using the Eq. (10) [36].

$$U_1 = n_1 n_2 + \frac{n_1(n_1+1)}{2} - R_1 \quad (10)$$

where R_1 is the sum of the ranks of group 1.

The ANOVA for multi-group comparison like threshold values, can be represented by Eq. (11) [36]. The one-way F- F-statistics

$$F = \frac{\text{Between-group MS}}{\text{Within-group MS}} = \frac{\frac{1}{g-1}\sum_{k=1}^{g} n_k(\bar{x}_k - \bar{x})^2}{\frac{1}{N_{\text{tot}}-g}\sum_{k=1}^{g}\sum_{i=1}^{n_k}(x_{ki} - \bar{x}_k)^2} \quad (11)$$

The differences observed in graph measures (degree centrality and clustering coefficient) are unlikely to be due to chance and, as indicated by a p-value < 0.05, represent a statistically significant difference between ictal and normal states. The reliability of our method is enhanced by smaller p-values (p < 0.01 or p < 0.001), which provide even stronger evidence of significant differences. The ability of our results to generate significant p-values for all samples ensured the robustness of the method and its potential for real-time seizure detection [21], [22], [23]. For temporal dynamics, to capture time-varying connectivity, we define sliding windows of length L samples with step s. For window w spanning t_w to $t_w + L - 1$. The phase of the channel i, for the window size w can be represented by Eq. (12) [22].

$$\phi_i^{(w)}(t) = \arg\left(\mathcal{H}\{s_i(t)\}\right), t \in [t_w, t_w + L - 1] \quad (12)$$

Compute $\text{PLI}_{ij}^{(w)}$ and adjacency $A^{(\tau,w)}$. Then features $DC^{(w)}, C^{(w)}$ became a time series.

Manuscript received 29 September 2025; Revised 27 November 2025; Accepted 25 November 2025; Available online 10 December 2025
Digital Object Identifier (**DOI**): https://doi.org/10.35882/jeeemi.v8i1.1230

C. Pseudocode

INPUT: EEG CSV files (epochs), thresholds T_list = [0.05,0.1,0.15], parameters: bandpass f1,f2, z_th, alpha=0.05

FOR each epoch file:

1. Read data matrix S_raw (T x N)
2. Preprocess:
   S_bp = bandpass(S_raw, f1, f2)
   S_clean =notch_and_artifact_rejection(S_bp, z_th) # optional ICA
3. Compute instantaneous phase:
   for i in 1..N:
   phi_i(t) = angle(Hilbert(S_clean[:,i]))
4. Compute PLI matrix P (N x N):
   for i in 1..N:
   for j=i+1..N: P_ij = | mean(sign(sin(phi_i - phi_j))) |
   P_ji = P_ij
5. Optional surrogate test: compute P_surrogate distribution, set P_ij=0 if P_ij <= percentile 95(P_surrogate)
6. For each threshold tau in T_list:
   A_tau = (P >= tau) # adjacency
   Compute DC(i)=sum_j A_ij / (N-1), average -> mean_DC
   Compute C(i) per node, average -> mean_C
   Store (filename, tau, mean_DC, mean_C)

OUTPUT: Features table; graphs (per tau optional)

STATISTICS: For group comparison (Normal vs Ictal):

For each tau:

- Test normality -> if approx normal: t-test, else Mann-Whitney U
- For multiple tau groups: ANOVA + posthoc
- Report p-values, effect sizes, and correct for multiple comparisons

III. Result

Degree centrality values remained low and evenly distributed during regular EEG activity, indicating an even brain connection, without any dominant hubs. Owing to the moderate clustering coefficient, information exchange among different brain areas is both efficient and flexible. A sparse network with moderate connections, which is characteristic of a stable working network, can be visually represented in the Phase Lag Index (PLI) graphs as shown in Fig. 3. However, the ictal state displays a sudden spike in degree centrality for specific nodes, generating hyper-connected seizure hotspots that disrupt normal brain function. In addition, the clustering coefficient increased significantly, leading to localized clusters that inhibit normal information dissemination and trap neuronal activity. A tightly connected structure with over-synchronization, characterized by large hubs and tightly linked clusters, is disclosed by the graphical presentation of the ictal PLI graph, as shown in Fig. 3. (f) to (j).

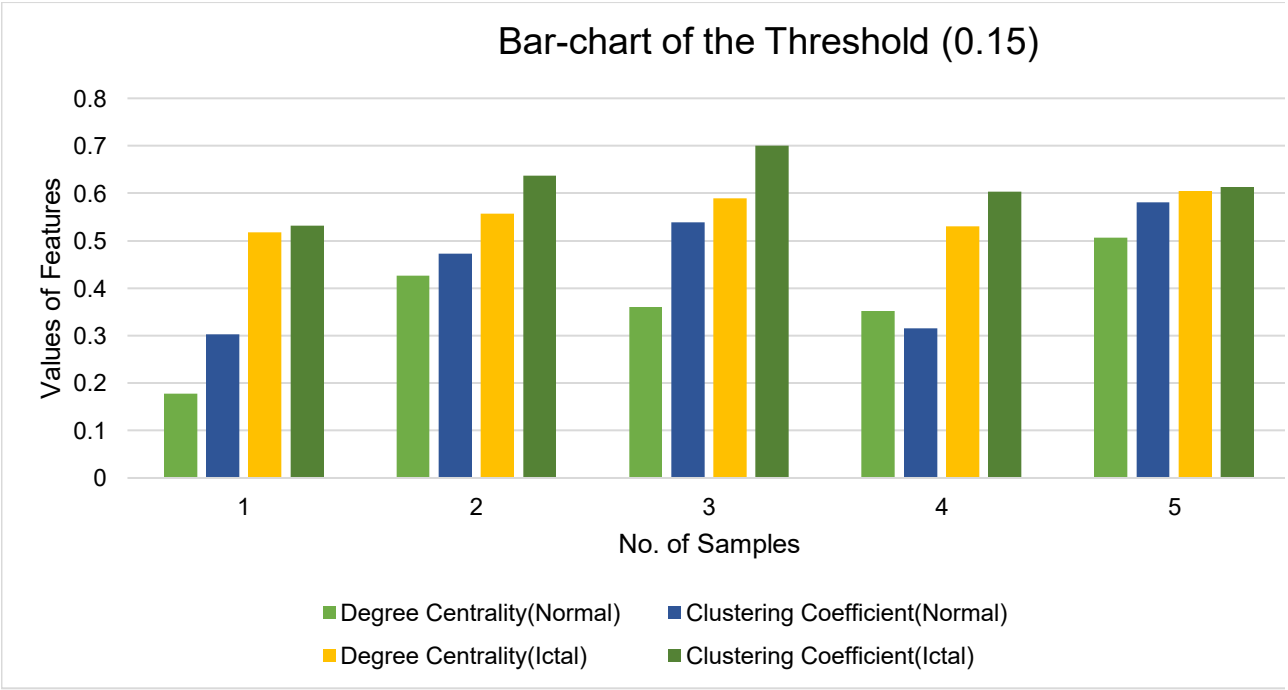

Fig. 4. Bar chart of the feature values for the Normal and Ictal state of the brain

Manuscript received 29 September 2025; Revised 27 November 2025; Accepted 25 November 2025; Available online 10 December 2025
Digital Object Identifier (**DOI**): https://doi.org/10.35882/jeeemi.v8i1.1230

Table 1. Features for all the samples, selecting the different threshold (0.05, 0.1 and 0.15)

Sample No.	Degree of Centrality (Normal)	Clustering Coefficient (Normal)	Degree of Centrality (Ictal)	Clustering Coefficient (Ictal)
Threshold Value 0.05				
1	0.632411	0.623678	0.786561	0.797933
2	0.798419	0.802363	0.853755	0.850185
3	0.711462	0.745839	0.841897	0.846789
4	0.762846	0.771816	0.833992	0.869143
5	0.802372	0.823175	0.885375	0.886052
Threshold value 0.1				
1	0.328063	0.384342	0.640316	0.649804
2	0.636364	0.629232	0.703557	0.708877
3	0.509881	0.638057	0.695652	0.746439
4	0.573123	0.597656	0.664032	0.750857
5	0.628458	0.651124	0.731225	0.724549
Threshold Value 0.15				
1	0.177866	0.302616	0.517787	0.53159
2	0.426877	0.472564	0.557312	0.636926
3	0.359684	0.538886	0.588933	0.699623
4	0.351779	0.315808	0.529644	0.602989
5	0.505929	0.580277	0.604743	0.613078

Table 2. Statistical Test Results to check the Significance of the proposed method

Threshold Value	Degree of Centrality	Clustering Coefficient	p-Value for Degree of Centrality	p-Value for Clustering Coefficient
T-Test				
0.05	-2.77571	-2.54343	0.024083	0.034526
0.1	-2.585404321	-2.568445236	0.032343378	0.033207781
0.15	-3.43936	-2.77227	0.008832	0.024212
ANOVA Test				
0.05	7.704571	6.46903	0.024083	0.034526
0.1	6.684315503	6.596910929	0.032343378	0.033207781
0.15	11.8292	7.685456	0.008832	0.024212
Mann-Whitney U Test				
0.05	2	2	0.031746	0.031746
0.1	0	1	0.007936	0.015873016
0.15	0	2	0.00793	0.031746

These alterations, transitioning from a dispersed to an extremely centralized network, underscore the abnormal connectivity patterns in the ictal state. These graph-based features are essential indicators for EEG-based epileptic seizure detection because they allow us to accurately identify seizures by examining the degree of centrality and clustering coefficient.

At three distinct PLI thresholds (0.05, 0.1, and 0.15), the graphs show how degree centrality and clustering coefficient vary among samples for both normal and ictal states, as shown in Tables 1. The reliability of graph-based measures for seizure detection improves as the threshold increases, as the discriminant power between the normal and ictal states becomes more pronounced. The bar chart shown in Fig. 4. can be plotted to compare the features of the normal and ictal states and provide more insight into the differences between the two brain states. We can directly observe that the Values of Degree centrality and Clustering coefficient in the ictal state are higher than in the normal state, as shown in Fig. 4.

Manuscript received 29 September 2025; Revised 27 November 2025; Accepted 25 November 2025; Available online 10 December 2025
Digital Object Identifier (**DOI**): https://doi.org/10.35882/jeeemi.v8i1.1230

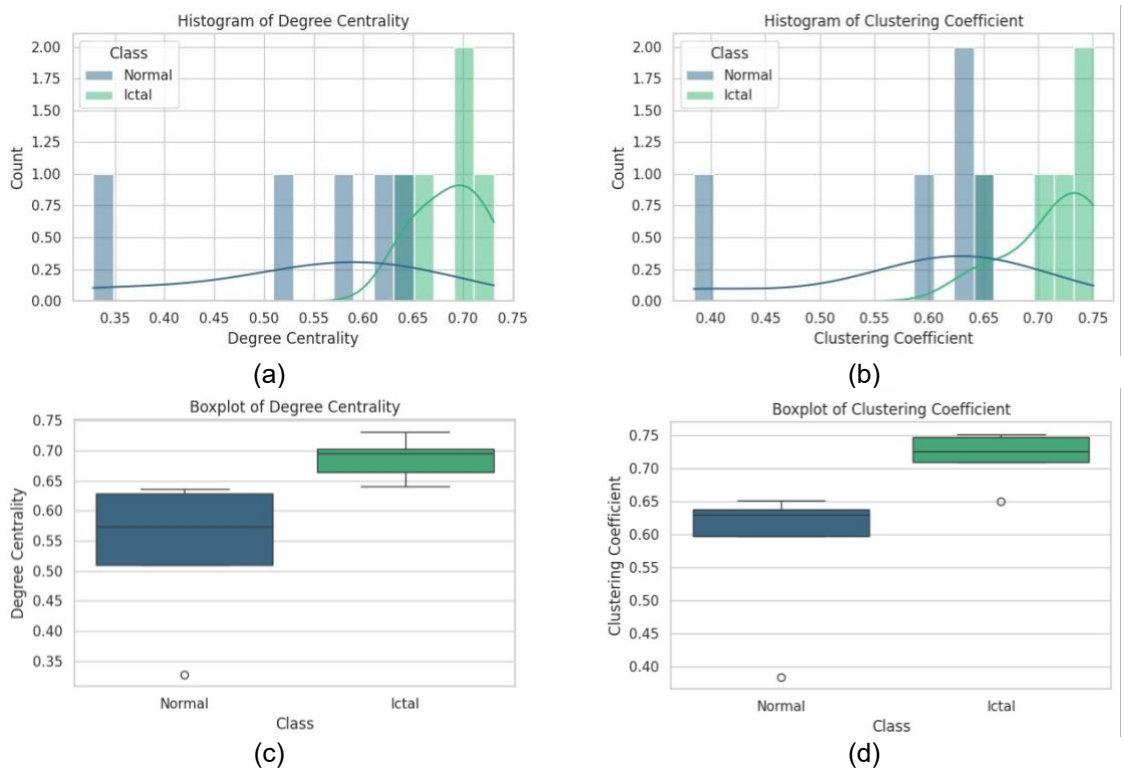

Fig. 5. Feature with Normal and Ictal Class (a) Histogram of Degree Centrality, (b) Histogram of Clustering Coefficient, (c) Box Plot of Degree Centrality, (d) Box Plot of Clustering Coefficient

The histograms in Fig. 5. (a) and (b) show clear peaks that attest to their efficacy in seizure detection, illustrating the distribution of the degree centrality and clustering coefficient across normal and ictal EEG states. Degree centrality values were noticeably greater in the ictal state, suggesting the development of seizure hubs with hyper-connected EEG channels. Similarly, as isolated clusters that interfere with regular brain transmission form, the clustering coefficient increases. This is further supported by the boxplots shown in Fig. 5. (c) and (d), which indicate increased variability and stronger synchronization during seizures, displaying a higher median and wider interquartile range (IQR) in the ictal state. The impact of seizure activity on brain networks is further supported by the occurrence of outliers in the ictal state, highlighting significant variations in connectivity.

Graph-theoretical metrics obtained from EEG-based functional brain networks were used to assess the proposed method, with particular emphasis on degree centrality and clustering coefficient as important markers of epileptic activity. We used a mix of T-tests, Analysis of Variance (ANOVA), and the Mann-Whitney U test across all threshold levels and datasets to statistically validate the discriminative potential of these features between normal and ictal states. The values of graph metrics showed significant differences between the two brain states, as shown in Tables 1, 2, and 3. In a few of the assessed samples, the p-value was < 0.05 in all statistical tests, indicating significant results across all frameworks of seizure detection. The T-test, ANOVA, and Mann-Whitney U test are appropriate for data that are not regularly distributed. Additionally, many samples attained more reliable criteria of $p < 0.01$, confirming the potency and reliability of these abilities in describing the ictal state of the brain. The T-test and ANOVA results further support these conclusions. ANOVA establishes statistically significant variance by offering a more comprehensive comparison across several groups and thresholds, whereas the t-test verifies substantial mean differences between normal and ictal circumstances. The reliability and strength of our proposed method are underscored by the consistently low p-values in multiple statistical tests. There is a clear demarcation in the graph characteristics for the distribution of ictal and normal states, as illustrated in the following plots and figures, confirming the statistical results. The quantitative results are supported by this visual distinction, which enhances the interpretability and therapeutic implications.

Together, these findings show that degree centrality and clustering coefficient are strong biomarkers for seizure detection when derived from Phase Lag Index (PLI)-based brain networks. Compared with complex machine learning or deep learning models, which often

Manuscript received 29 September 2025; Revised 27 November 2025; Accepted 25 November 2025; Available online 10 December 2025
Digital Object Identifier (**DOI**): https://doi.org/10.35882/jeeemi.v8i1.1230

suffer from interpretability issues, our method is a more transparent, computationally efficient, and clinically relevant alternative. Robust statistical verification and graphically based confirmation complement each other to ensure that the proposed technique attains high dependability and has implications for offline and real-time seizure-detection systems.

IV. Discussion

In our study, we started with the Children's Hospital Boston-MIT (CHB-MIT) EEG dataset, which contains raw files in the European data format (EDF) of 1–2 h of time line. The signals were then converted to CSV files for further analysis. Before performing the analysis and feature extraction, the necessary steps of raw data processing were applied to remove power-line noise, movement artifacts, and eye-blink noise using appropriate filtering techniques. Subsequently, we extracted the epochs representing normal and ictal states, as mentioned in the original dataset. Phase Lag Index analysis was then performed to quantify functional connectivity. These preprocessed, well-defined epochs provided a basis for feature extraction and subsequent statistical evaluation [8], [12].

Using PLI, we obtained functional connectivity metrics and analyzed the brain's network organization using graph-theoretical measures. The two functional features, degree centrality and clustering coefficient, were extracted because they capture both the global integration and local segregation properties of the brain network. Degree centrality quantifies a node's (EEG electrode's) importance in the network by counting its direct connections. Mathematically, for a node i, degree centrality can be represented using Eq. (7) [31], [32]. The other feature, the clustering coefficient, measures the extent of local interconnectedness among neighboring nodes and thereby reflects the segregation of neural assemblies. It can be derived using Eq. (8). where k_i is the number of neighbors of node i, and e_i is the number of existing connections among those neighbors.

During ictal states, clustering coefficients were higher, indicating abnormally strong local synchronization compared to the balanced patterns observed in normal states. To check the differences were not random, we employed statistical testing. The independent sample T-test and Mann-Whitney U test were used to confirm significant differences between normal and ictal states. Moreover, ANOVA was performed to examine variations across multiple PLI thresholds (0.05, 0.1, and 0.15). The adoption of a p-value threshold of 0.05 enabled us to ignore the null hypothesis, which confirms that the observed changes in degree centrality and clustering coefficient are statistically significant, as shown in Table 2 [21], [33]. The use of multiple thresholds (0.05, 0.1, and 0.15) ensured robustness in network connectivity. Lower thresholds (0.05) allowed the detection of weaker, subtle connections, and higher thresholds (0.15) retained only the strongest and most reliable links. This multi-threshold approach confirmed that the results were not biased by a single threshold but were consistent across various network densities.

The proposed method demonstrates that the higher values of degree centrality and clustering coefficient are higher in the ictal state than in the normal state. From this study, we can say that seizures are characterized by the emergence of hyper-synchronous hubs and logically over-connected clusters, supporting the rigid and less flexible brain network topology. In contrast, normal brain states exhibit a more distributed and adaptive network organization. The results we acquired highlight the potential of PLI-based graph measures in EEG-driven seizure detection, which contributes to the development of a reliable seizure detection system [32], [34].

To summarize the proposed method based on the computational complexity and practical advantages, the PLI computation is beneficial, considering that each epoch costs $O(N^2T)$ where T is epoch length (phase computation via Hilbert is $O(NT\log T)$ if using FFT-based on Hilbert). Now if we discuss graph metrics, for binary graphs with E edges; degree is $O(N+E)$ (Linear), clustering naïve $O(\sum_i k_i^2)$ where k_i are degrees; for sparse graphs, this is efficient. Modularity and community detection vary by algorithm. Deep learning requires $O(M \cdot \text{params} \cdot T)$ training complexity and many labeled examples. Our method is computationally cheaper, interpretable, and feasible for small datasets. The detailed comparison of the present study is shown in the Table.3

The automatic detection and prediction of epileptic seizures using electroencephalography (EEG) has evolved significantly in recent years, with advancements in methodologies ranging from functional connectivity analysis to deep learning and graph-based frameworks. The core challenges lie in maintaining accuracy, interpretability, and computational feasibility to achieve clinically meaningful systems. Functional connectivity has been broadly studied as a means of capturing pathological synchronization in epilepsy. Mao et al. (2022) stated that the frontotemporal phase lag index (PLI) correlated with seizure severity in patients with temporal lobe epilepsy, justifying PLI as a robust biomarker of network abnormalities during ictal events [24]. Complementing this, Coa et al. (2022) demonstrated the effects of vagal nerve stimulation in drug-resistant epilepsy and showed that estimated EEG functional connectivity and the aperiodic component could be

Manuscript received 29 September 2025; Revised 27 November 2025; Accepted 25 November 2025; Available online 10 December 2025
Digital Object Identifier (**DOI**): https://doi.org/10.35882/jeeemi.v8i1.1230

Table 3. The comparison of available research with the proposed method

Study	Dataset	Features	Selection	Classifier / Model	Key Findings	Strengths	Limitations
Liu et al. (2024) [28]	CHB-MIT	Spatiotemporal EEG features	Not graph-based	Pseudo-3D CNN	Effective seizure prediction with fused temporal & spatial features	Strong accuracy, good feature fusion	Requires large datasets, high computational load
Zhang et al. (2024) [29]	Multiple EEG datasets reviewed	Survey of ML/DL methods	Some studies used graph theory	– (review paper)	Deep learning shows strong performance, but interpretability is a challenge	Provides holistic comparison across methods	No experimental validation (review only)
Zhang et al. (2024) [30]	CHB-MIT, clinical datasets	Event-driven spiking features	Not graph-based	Spiking Neural Networks (SNN)	High generalizability across patients; energy-efficient	Suitable for wearable devices	Less interpretable than graph-based methods
Hajisafi et al. (2024) [27]	CHB-MIT	Dynamic functional connectivity graphs	Evolving graph embeddings	Graph Neural Networks (GNNs)	Captures spatiotemporal evolution in EEG networks	High performance, captures dynamics	Preprint stage; computationally heavy
Mao et al. (2022) [24]	Clinical EEG	Phase Lag Index (PLI)	Frontotemporal connectivity	Statistical correlation	PLI correlates with seizure severity	Clinically relevant biomarker	Limited to severity analysis, not prediction
Coa et al. (2022) [25]	Clinical EEG (drug-resistant epilepsy)	Functional connectivity + aperiodic component	Graph-based analysis	Functional connectivity measures	VNS modulates EEG connectivity	Shows the neuromodulation impact	Focused on stimulation, not direct prediction
Jia et al. (2022) [26]	CHB-MIT	Graph-based EEG features	Graph connectivity	Graph Convolutional Network (GCN)	GCN improves prediction efficiency	Strong predictive power	Deep model, lower interpretability
Proposed Study (2025)	CHB-MIT (23 bipolar channels)	Phase Lag Index (PLI) → minimizes volume conduction	Degree Centrality, Clustering Coefficient	Statistical tests (T-test, ANOVA, Mann-Whitney U) + interpretable analysis	Significant rise in graph metrics during ictal; hyperconnected hubs observed	Computationally efficient, interpretable, suitable for real-time applications	Limited to graph-based biomarkers; needs multimodal validation

Manuscript received 29 September 2025; Revised 27 November 2025; Accepted 25 November 2025; Available online 10 December 2025
Digital Object Identifier (**DOI**): https://doi.org/10.35882/jeeemi.v8i1.1230

highlight the clinical relevance of connectivity-based markers, not only for diagnosis but also for monitoring therapeutic interventions. Building on connectivity measures, graph-theoretical models have been employed to characterize topological changes in epileptic brain networks. Jia et al.(2022) used efficient graph convolutional networks (GCNs) to scalp EEG for seizure prediction, confirming that graph-based representations enhance predictive performance by modeling spatial and temporal relationships across channels [26]. Using a similar approach, Hajisafi et al. (2024) proposed a NeuroGNN, which is a dynamic graph neural network framework capable of identifying evolving connectivity patterns to achieve a higher classification accuracy. Such results show a strong predictive power, but the architectural complexity and dependence on large-scale computational power hinder real-time detection of epilepsy [27].

In recent years, deep learning models have achieved significant improvements in seizure detection accuracy by leveraging spatiotemporal information in EEG signals. Liu et al. (2024) proposed an approach based on BiConvLSTM, which was a pseudo three-dimensional approach that fuses handcrafted and learned features to predict seizures. Additionally, these methods require significant computational power, which may hinder their clinical deployment [28]. A detailed review by Zhang et al. (2024) highlights these trade-offs, mentioning that while deep neural networks outperform conventional signal processing methods, their “black-box” nature restricts interpretability and clinical trust [29]. To showcase efficiency concerns, Zhang et al. (2024) explored spiking neural networks for cross-patient seizure detection, confirming energy-efficient computation suitable for wearable devices. However, the accuracy gap related to conventional deep learning methods remains a limitation [30].

Considering these factors, earlier research highlights two prevailing directions. The first is based on biologically grounded measures, such as PLI and connectivity indices, which provide interpretability but may be underutilized in recent computational frameworks. The other method is based on deep learning, and GNN provides high accuracy, but it has high complexity and low transparency. Our study was conducted at the intersection of these paragons. The utility of PLI for functional connectivity networks, along with graph features such as degree centrality and clustering coefficient, shows a significant and consistent difference between normal and ictal states. If we compare GNN-based methods (Jia et al., 2022; Hajisafi et al., 2024), our approach is mathematically lightweight and requires no intensive training, making it more reliable for real-time applications [26], [27].

Moreover, by considering interpretable graph features, our method addresses the limitations of the black-box deep learning approach (Zhang et al., 2024) while retaining a strong discriminatory power. Thus, our approach provides an efficient, interpretable, and clinically relevant framework for seizure detection, complementing methods based on deep learning and connectivity [29]. The detailed comparison with the present study is shown in the Table. 3.

Although our approach was trained on randomly selected participants from the CHB-MIT dataset, its consistent performance across these scenarios indicates strong generalizability. Dependability and robustness are assured through the use of graph-based features and strict statistical validation. Although the analysis was performed offline, it provides a robust foundation for future real-time applications. While advanced filtering and artifact-removal methods may further enhance precision, subtle signal artifacts can still affect connectivity measures. Such features offer promising avenues for the development and refinement of the method to broader clinical environments.

V. Conclusion

The PLI-based approach for detecting the ictal state using a Graph Theory network provides a robust, interpretable framework. By converting CHB-MIT data from EDF to CSV, rigorously preprocessing the data, and analyzing appropriate epochs, we successfully constructed functional brain networks that highlighted connectivity changes related to seizures. The graph-theoretic features, namely degree centrality and clustering coefficient, capture the pathological hyper-synchronization and localized clustering characteristics of ictal states. The reliability and robustness of the proposed method were validated using statistical tests, including the t-test, ANOVA, and the Mann-Whitney U test, across different thresholding PLI levels (0.05, 0.1, and 0.15). Our study is computationally efficient, interpretable, and suitable for real-time seizure detection compared to deep learning techniques that require high training and processing power. The results show that graph-based analysis of functional connectivity is an efficient and potentially capable real-time or near-real-time seizure detection method, making it an alternative to established techniques in medical practice. For future aspects, our work is based on a single publicly available dataset, and the method can be verified by exploring dynamic graph metrics, adaptive thresholding, multi-patient generalization, and real-time deployment in clinical and wearable EEG platforms.

Manuscript received 29 September 2025; Revised 27 November 2025; Accepted 25 November 2025; Available online 10 December 2025
Digital Object Identifier (**DOI**): https://doi.org/10.35882/jeeemi.v8i1.1230

Acknowledgment

The authors would like to express sincere gratitude to the Department of Electronics and Communication of CSPIT, Charsadda University, for their continuous support. The authors also acknowledge the support from the online data providers CHB-MIT.

Funding

No funding was received from any of the agencies or organizations for this research.

Data Availability

The data used in this study are openly available in the PhysioNet repository: CHB-MIT Scalp EEG Database [https://physionet.org/content/chbmit/1.0.0/]. These data were used in compliance with the PhysioNet data use agreement.

Author Contribution

Ghansyamkumar Rathod has worked on the data preprocessing, feature extraction work, along with the literature review. The result analysis, along with statistical validation checking, was done by Dr. Hardik Modi.

Declarations

Ethical Approval

This study was based on the datasets provided by CHB-MIT, which were anonymized and hosted online on PhysioNet. Ethical approval for this study was not required because the CHB-MIT dataset was previously collected under ethical protocols approved by the Institutional Review Board (IRB) of Boston Children's Hospital and the Massachusetts Institute of Technology. All the data were collected in accordance with the principles of the Declaration of Helsinki.

Consent for Publication Participants.

Consent for publication was given by all participants

Competing Interests

The authors declare no competing interests.

References

[1] D. Pascual, D. Atienza, R. Wattenhofer, A. Amirshahi, A. Aminifar, and P. Ryvlin, "EpilepsyGAN: Synthetic epileptic brain activities with privacy preservation," IEEE Transactions on Biomedical Engineering, vol. 68, no. 8, pp. 2435–2446, Dec. 2020.

[2] K. S. Shekokar and S. Dour, "Automatic epileptic seizure detection using LSTM networks," World Journal of Engineering, vol. 19, no. 2, pp. 224–229, Aug. 2021.

[3] D. Liu, X. Dong, W. Zhou, and D. Bian, "Epileptic seizure prediction using attention augmented convolutional network," International Journal of Neural Systems, vol. 33, no. 11, Sept. 2023.

[4] S. Skaria and S. K. Savithriamma, "Automatic classification of seizure and seizure-free EEG signals based on phase space reconstruction features," Journal of Biological Physics, vol. 50, no. 2, pp. 181–196, Mar. 2024.

[5] I.B. Slimen, H. Seddik, Z. Mbarki, and L. Boubchir, "EEG epileptic seizure detection and classification based on dual-tree complex wavelet transform and machine learning algorithms," Journal of Biomedical Research, vol. 34, no. 3, p. 151, May 2020.

[6] G. Yogarajan et al., "EEG-based epileptic seizure detection using binary dragonfly algorithm and deep neural network," Scientific Reports, vol. 13, no. 1, Oct. 2023.

[7] Z. Huang et al., "EEG detection and recognition model for epilepsy based on dual attention mechanism," Scientific Reports, vol. 15, no. 1, Mar. 2025.

[8] Z. Wang, J. Zhang, Y. Zhao, and Y. He, "Phase lag index-based graph attention networks for detecting driving fatigue," Review of Scientific Instruments, vol. 92, no. 9, p. 094105, Sept. 2021.

[9] A. Mahajan, M. Sameer, and K. Somaraj, "Adopting artificial intelligence powered ConvNet to detect epileptic seizures," in Proc. IEEE Conf., 2021.

[10] Y. Gao, Y. Zhang, J. Liu, B. Gao, and Q. Chen, "Deep convolutional neural network-based epileptic electroencephalogram (EEG) signal classification," Frontiers in Neurology, vol. 11, May 2020.

[11] S. Sheykhivand, A. Farzamnia, A. Delpak, T. Y. Rezaii, and Z. Mousavi, "Automatic identification of epileptic seizures from EEG signals using sparse representation-based classification," IEEE Access, vol. 8, pp. 138834–138845, Jan. 2020.

[12] Q. Sun, Y. Liu, and S. Li, "Weighted directed graph-based automatic seizure detection with effective brain connectivity for EEG signals," Signal, Image and Video Processing, vol. 18, no. 1, pp. 899–909, Oct. 2023.

[13] Y. Tang, Q. Wu, H. Mao, and L. Guo, "Epileptic seizure detection based on path signature and Bi-LSTM network with attention mechanism," IEEE Transactions on Neural Systems and Rehabilitation Engineering, vol. 32, pp. 304–313, Jan. 2024.

[14] X. Wang et al., "One dimensional convolutional neural networks for seizure onset detection using long-term scalp and intracranial EEG," Neurocomputing, vol. 459, pp. 212–222, June

Manuscript received 29 September 2025; Revised 27 November 2025; Accepted 25 November 2025; Available online 10 December 2025
Digital Object Identifier (**DOI**): https://doi.org/10.35882/jeeemi.v8i1.1230

2021.

[15] F. Hassan, S. M. Qaisar, and S. F. Hussain, "Epileptic seizure detection using a hybrid 1D CNN-machine learning approach from EEG data," Journal of Healthcare Engineering, vol. 2022, pp. 1–16, Nov. 2022.

[16] C. Tian and F. Zhang, "EEG-based epilepsy detection with graph correlation analysis," Frontiers in Medicine, vol. 12, Mar. 2025.

[17] Y. Yan et al., "Functional connectivity alterations based on the weighted phase lag index: An exploratory electroencephalography study on Alzheimer's disease," Current Alzheimer Research, vol. 18, no. 6, pp. 513–522, May 2021.

[18] N. Feng, B. Zhou, H. Wang, and F. Hu, "Motor intention decoding from the upper limb by graph convolutional network based on functional connectivity," International Journal of Neural Systems, vol. 31, no. 12, Oct. 2021.

[19] W. Bomela, J. S. Li, S. Wang, and C. A. Chou, "Real-time inference and detection of disruptive EEG networks for epileptic seizures," Scientific Reports, vol. 10, no. 1, May 2020.

[20] Y. Pan et al., "Epileptic seizure detection with hybrid time-frequency EEG input: A deep learning approach," Computational and Mathematical Methods in Medicine, vol. 2022, suppl. 2, pp. 1–14, Feb. 2022.

[21] N. Zhao, X. Zhou, S. Yang, H. Wang, J. Wang, and T. Luo, "A novel method to identify key nodes in complex networks based on degree and neighborhood information," Applied Sciences, vol. 14, no. 2, p. 521, Jan. 2024.

[22] K. Zhang et al., "Towards identifying influential nodes in complex networks using semi-local centrality metrics," Journal of King Saud University – Computer and Information Sciences, vol. 35, no. 10, p. 101798, Oct. 2023.

[23] Y. V. Nandini, T. J. Lakshmi, M. K. Enduri, and H. Sharma, "Link prediction in complex networks using average centrality-based similarity score," Entropy, vol. 26, no. 6, p. 433, May 2024.

[24] L. Mao et al., "Frontotemporal phase lag index correlates with seizure severity in patients with temporal lobe epilepsy," Frontiers in Neurology, vol. 13, Dec. 2022.

[25] R. Coa et al., "Estimated EEG functional connectivity and aperiodic component induced by vagal nerve stimulation in patients with drug-resistant epilepsy," Frontiers in Neurology, vol. 13, Nov. 2022.

[26] M. Jia et al., "Efficient graph convolutional networks for seizure prediction using scalp EEG," Frontiers in Neuroscience, vol. 16, Aug. 2022.

[27] A. Hajisafi, H. Lin, Y. Y. Chiang, and C. Shahabi, "Dynamic GNNs for precise seizure detection and classification from EEG data," in Proc. Pacific-Asia Conf. Knowledge Discovery and Data Mining (PAKDD), vol. 14648, pp. 207–220, Jan. 2024.

[28] X. Liu et al., "Epileptic seizure prediction based on EEG using pseudo-three-dimensional CNN," Frontiers in Neuroinformatics, vol. 18, Mar. 2024.

[29] X. Zhang, X. Zhang, Q. Huang, and F. Chen, "A review of epilepsy detection and prediction methods based on EEG signal processing and deep learning," Frontiers in Neuroscience, vol. 18, Nov. 2024.

[30] Z. Zhang et al., "Efficient and generalizable cross-patient epileptic seizure detection through a spiking neural network," Frontiers in Neuroscience, vol. 17, Jan. 2024.

[31] K. Song, J. Li, Y. Zhu, F. Ren, L. Cao, and Z. G. Huang, "Altered small-world functional network topology in patients with optic neuritis: A resting-state fMRI study," Disease Markers, vol. 2021, no. 37, pp. 1–9, June 2021.

[32] H. Javaid, E. Kumarnsit, and S. Chatpun, "Age-related alterations in EEG network connectivity in healthy aging," Brain Sciences, vol. 12, no. 2, p. 218, Feb. 2022.

[33] M. L. M. Zimmermann et al., "The relationship between pathological brain activity and functional network connectivity in glioma patients," Journal of Neuro-Oncology, vol. 166, no. 3, pp. 523–533, Feb. 2024.

[34] T. Wadhera and M. Mahmud, "Brain functional network topology in autism spectrum disorder: A novel weighted hierarchical complexity metric for electroencephalogram," IEEE Journal of Biomedical and Health Informatics, pp. 1–8, Jan. 2022.

[35] Sen, Dipanwita, Bhupati Bhusan Mishra, and Prasant Kumar Pattnaik. "A review of the filtering techniques used in EEG signal processing." In 2023 7th International Conference on Trends in Electronics and Informatics (ICOEI), pp. 270-277. IEEE, 2023.

[36] Kardys, Isabella, Sanne Hoeks, Ron van Domburg, Mattie Lenzen, and Eric Boersma. "Tools and techniques–statistics: analysis of continuous data using the t-test and ANOVA." EuroIntervention J Eur Collab Work Group Interv Cardiol Eur Soc Cardiol 9, no. 6 (2013): 765-767.

Manuscript received 29 September 2025; Revised 27 November 2025; Accepted 25 November 2025; Available online 10 December 2025
Digital Object Identifier (**DOI**): https://doi.org/10.35882/jeeemi.v8i1.1230

Author Biography

Ghansyamkumar Rathod has completed a Bachelor of Engineering in Electronics from Birla Vishvakarma Mahavidyalaya Engineering College, Sardar Patel University (SPU) in 2007 and a Master of Engineering in Communication from G.H.Patel Institute of Technology, Gujarat Technological University (GTU) in 2012. He is pursuing a Ph.D from Charotar University of Science and Technology. He has more than 17 years of teaching experience and has expertise in the field of biomedical instrumentation and signal processing, sensors, transducers, analog electronics, network analysis, linear integrated circuits, and robotics. He had guided many major and minor projects of undergraduate students. He is keen to develop digital study materials for his students for easy access during their studies. https://orcid.org/0000-0001-9613-2988

Dr. Hardik Modi has completed a Bachelor of Engineering in Electronics and Communication from Sardar Patel University (SPU) in 2005, a Master of Engineering in Communication Systems from Dharmsinh Desai University (DDU) in 2007 and aDoctorate of Philosophy from Charotar University of Science and Technology (CHARUSAT) in 2016. He is Associate professor at CSPIT. He has more than 19 years of teaching experience. He has expertise in the field of VLSI, Circuits and Networks, Signal Processing, and Embedded systems. He had guided many UG and PG students for minor and major projects. He had supervised many PhD research projects. https://orcid.org/0000-0002-1847-4234

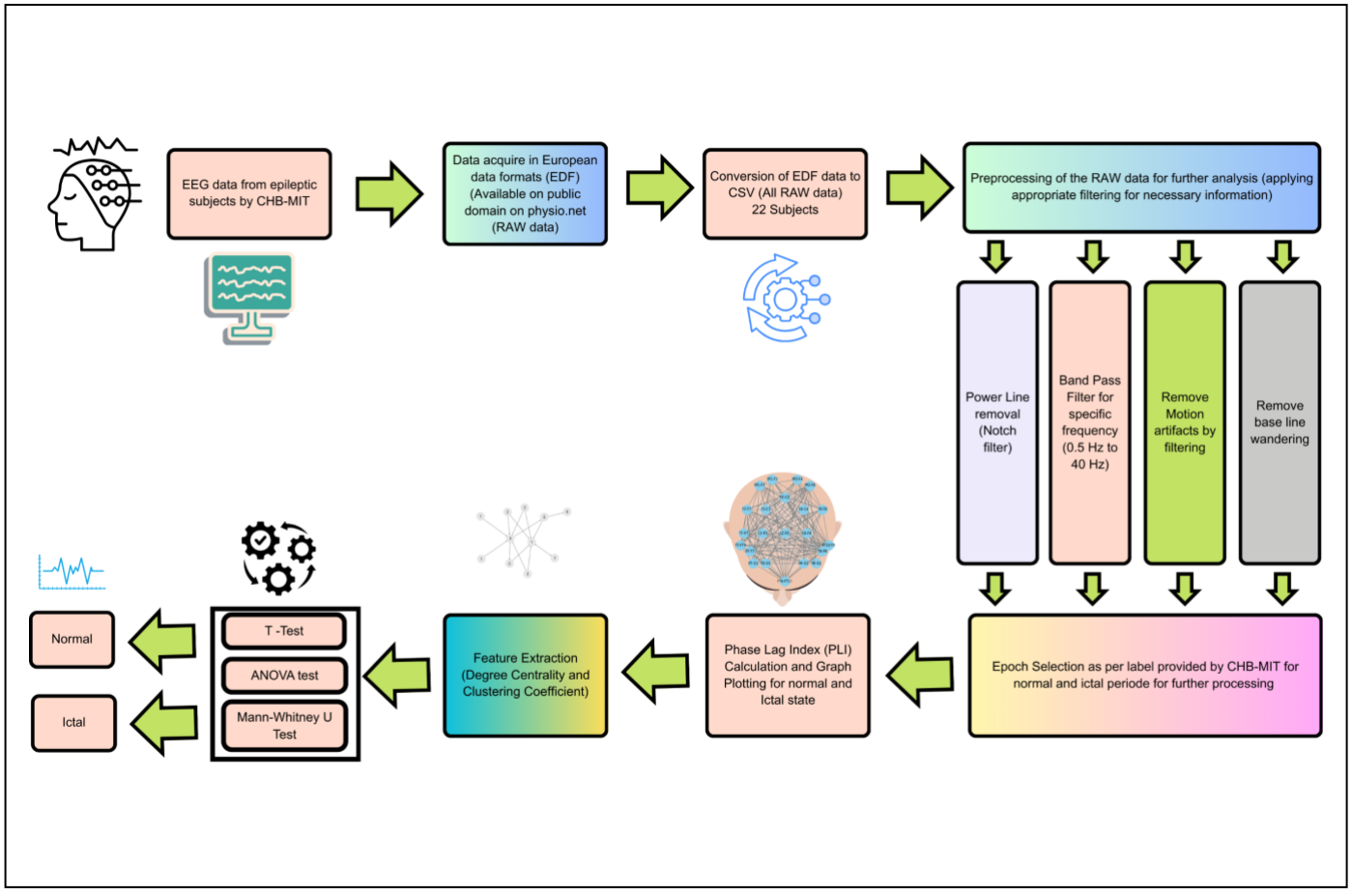

Manuscript received 29 September 2025; Revised 27 November 2025; Accepted 25 November 2025; Available online 10 December 2025
Digital Object Identifier (**DOI**): https://doi.org/10.35882/jeeemi.v8i1.1230